Design of 57.5 MHz CW RFQ Structure for the Rare Isotope Accelerator Facility[1]

P. N. Ostroumov, A.A. Kolomiets[2]

Physics Division, Argonne National Laboratory, 9700 S. Cass Avenue, Argonne, IL, 60439

D.A. Kashinsky, S.A. Minaev, V.I. Pershin, T.E. Tretyakova, S.G. Yaramishev

Institute of Theoretical and Experimental Physics, Moscow 117259, Russia

Abstract

The Rare Isotope Accelerator (RIA) facility includes a driver linac for production of 400 kW CW heavy-ion beams. The initial acceleration of heavy-ions delivered from an ECR ion source can be effectively performed by a 57.5 MHz four-meter long RFQ. The principal specifications of the RFQ are: 1) formation of extremely low longitudinal emittance; 2) stable operation over a wide range of voltage for acceleration of various ion species needed for RIA operation; 3) simultaneous acceleration of two-charge states of uranium ions.

CW operation of an accelerating structure leads to a number of requirements for the resonators such as high shunt impedance, efficient water cooling of all parts of the resonant cavity, mechanical stability together with precise alignment, reliable rf contacts, a stable operating mode and fine tuning of the resonant frequency during operation. To satisfy these requirements a new resonant structure has been developed.

This paper discusses beam dynamics and electrodynamics design of the RFQ cavity, as well as, some aspects of the mechanical design of this low-frequency CW RFQ.

Introduction

The initial acceleration of heavy-ion beams in the driver linac of the Rare Isotope Accelerator (RIA) Facility [1] will be provided by room temperature RFQ operating at 57.5 MHz. The primary scope of the RFQ is the formation of low longitudinal emittance dual charge state uranium beams. Transverse emittance should remain unchanged and a high beam capture efficiency is required. In order to simplify the front end of multi-beam driver linac and accommodate different ion species from the ECR ion source the RFQ must operate at wide range of power levels. The basic RFQ design specifications are listed in Table 1. Several types of resonant structures have been analyzed in order to satisfy all specifications. As a result we propose an original RFQ structure which combines advantages of the four-vane and split-coaxial structures. Four-vane RFQs provide high shunt-impedances while split-coaxial structures have extremely good mode separation.

Beam dynamics design

The shape of the RFQ vanes (or electrodes) was using the code DESRFQ [2]. In this code the accelerating cell is determined as a distance between the cross-sections with exact quadrupole symmetry of electrodes. These cross-sections are equivalent to the accelerating gap centers in a standard drift tube linac. The code calculates iteratively length of *i-th* cell, L_{ci}, for a given

---

[2] On leave from Institute of Theoretical and Experimental Physics, Moscow.

modulation factor, m_i, so that reference particle exits a cell at given synchronous phase, φ_{si}. An additional condition is required in order to calculate the RFQ parameters, m_i and φ_{si}, in each cell at given peak surface field. This condition is discussed below.

Table 1. Initial requirements for RFQ design

Duty cycle	100%
Operating frequency	57.5 MHz
Resonant cavity	Based on the split-coaxial structure
Input particle velocity	0.00507 c
Design charge to mass ratio	28.5/238
Charge to mass ratio of accelerated ions	28/238; 29/238
Length of the RFQ vanes	~ 4 m
Output beam energy	~200 keV/u
Peak field at electrode surface	$\leq$ 1.25 Kilpatrick units
Normalized transverse emittance	0.5 π mm mrad
Longitudinal emittance at the exit of RFQ for 99.9% of particles	$\leq$ 2 keV/u·nsec

The code DESRFQ calculates electric field distributions in a cell for each iteration using the modified version of the code POLE1 [3]. Eight coefficients of the Fourier-Bessel series describing potential distribution in a cell with given shape of the electrodes are calculated:

$$U(r,\psi,z) = -\frac{U_l}{2}\left[F_0(r,\psi) + \sum_{n=1}^{\infty} F_n(r,\psi)\sin(2n-1)kz \right]$$

$$F_0(r,\psi) = \sum_{s=0}^{\infty} B_s \left(\frac{r}{R_0}\right)^{2(2n-1)} \cos(2(2s+1)\psi) \qquad (1)$$

$$F_n(r,\psi) = \sum_{s=0}^{\infty} A_{ns} I_{4s}\left[(2n-1)kr\right]\cos 4s\psi,$$

where F_n, B_s and A_{ns} are the coefficients of the Fourier-Bessel expansion, $k = 2\pi/\beta\lambda$, β is the relative ion velocity, λ is the wavelength of rf field, and R_0 is the characteristic (or average) radius of the RFQ electrodes. The vane tip is a semicircle with the radius $R_e=0.75R_0$. The distance from the RFQ axis to the vane tip in each i-th cell is determined by sinusoidal curve with respect to the longitudinal coordinate z:

$$x_i = R_0\left(1 + \frac{m_i-1}{m_i+1}\sin kz\right)$$

$$y_i = R_0\left(1 - \frac{m_i-1}{m_i+1}\sin kz\right)$$

The code DESRFQ directly calculates the coefficients of the Fourier-Bessel series (1) for sinusoidal shape of the vane tips.

If the peak surface field is specified, the stability region of transverse oscillation in the RFQ can be calculated for the given characteristic R_0. Figure 1 shows the phase advance and normalized acceptance in the transverse planes as a function of R_0. The curves were calculated for $R_e/R_0 = 0.75$. Choosing $R_0 = 0.6$ mm we can obtain a transverse acceptance which is three times larger than the

expected beam emittance from the ion source and provide sufficiently strong transverse focusing. For this value of R_0 the maximum value ρ_{max} of the modulus of the Floquet function $\rho(t)$ is small enough and beam envelope, $r_{max} = \sqrt{\lambda \cdot \varepsilon_n} \, \rho_{max}$, is about 2.3 mm which results in motion of the particles in linear focusing fields. The matched beam parameters at the RFQ entrance were determined by inverse transformation of $\rho(t)$ and $\dfrac{d\rho(t)}{dt}$ through six-cell matching sections where the distance from axis to the vane tip is given by,

$$x(z) = R_0 \, \frac{1}{sin\left(\pi \dfrac{z - 0.5}{12 \, L_{c0}} \right)} \; .$$

As was discussed in our previous work [4], to obtain the lowest possible longitudinal emittance of two charge state beams, a multi-harmonic buncher must be used upstream of the RFQ. The ion beam distribution in the longitudinal phase space at the RFQ entrance is determined by the four-harmonic buncher and is shown in Fig. 2. The central part of the distribution contains more than 80% of the particles within a phase width of $\pm 25^0$. The main goal of beam dynamics design is to accept the core of the initial distribution and reliably eliminate halo particles from the acceleration process. This can be done if the acceleration starts with small size separatrix and its length is kept constant along the RFQ. The condition

$$\frac{T \sin \varphi_s}{\beta^2} = const \tag{2}$$

ensures a conservation all particle trajectories in phase space in the linear approximation; T is the acceleration efficiency. However, the situation is more complicated due to the strong coupling of the longitudinal and transverse motions in the front end of the RFQ which is inherent in heavy-ion RFQs. The Hamiltonian for longitudinal motion in an RFQ can be expressed as [5]:

$$H(\Delta z, \Delta \beta) = \frac{c \Delta \beta^2}{2} + \frac{qeU_0 T}{\pi A W_e}\left(k\Delta z \, cos \, \varphi_s - I_0^2\left(\frac{kR}{2}\right) sin(k\Delta z - \varphi_s) \right), \tag{3}$$

where Δz, Δp are particle coordinates with respect to the reference particle in the phase space, qe is the ion charge, $W_e = m_e c^2$, m_e is the atomic unit mass, A is the mass number, c is the speed of light, U_0 is the vane-to-vane voltage, R is the average amplitude of transverse oscillations, and I_0 is the modified Bessel function. In the front end of the RFQ the term $I_0(kR/2)$ is not small and the Hamiltonian strongly depends on amplitude of transverse oscillations. Figure 3 shows the separatrices calculated for an initial value of the particle velocity of $\beta = 0.00507$ for different amplitudes of the transverse oscillations. The initial values of T and φ_s can be chosen to accept central dense area of the initial distribution into the separatrix corresponding to $R=0$. However, there are particles with large transverse amplitudes. These particles are captured for acceleration and have large amplitude longitudinal oscillations. Obviously, they form a halo in the longitudinal phase space. As is expected the total longitudinal emittance can significantly exceed the emittance of the central part containing 80 – 85% of particles. An obvious way to weaken the coupling between the transverse and longitudinal motions is to increase the injection energy or wavelength of the rf. However, increasing these parameters will impact on the cost of RFQ.

To avoid resonant conditions for the frequency of transverse and longitudinal oscillations, the following condition must be satisfied in the RFQ [5]:

$$\frac{\Omega_l}{\Omega r} < \frac{1}{I_0\left(\frac{ka}{2}\right)}$$

where Ω_l and Ω_r are the frequencies of small longitudinal and transverse oscillations respectively. In our design this condition is fulfilled along the whole RFQ.

Because the external multi-harmonic buncher produces short bunches at the RFQ entrance, the synchronous phase of the RFQ may be kept constant along the structure. The initial modulation was chosen to minimize the amplitude of energy oscillations. Then the modulation factor varies according to relation (2) along the structure up to the point where $\beta = 0.017$. Downstream of this point the modulation factor is kept constant in order to maintain a high transverse phase advance.

The final parameters of the RFQ are presented in Table 2 and Fig. 4 and 5.

Table 2. Main design RFQ parameters

Average radius R_0	0.6 cm
Vane tip radius R_e	0.45 cm
Vane-to-vane voltage U_0	68.5 kV
Maximum field on the vane surface E_{max}	140 kV/cm
Synchronous phase φ_s	-25^0
Beam energy	199.0 keV/u
Modulation factor	$1.09 \div 1.765$
Aperture	0.43 cm
Phase advance of transverse oscillations σ_0	$44^0 - 41^0$
Reduced transverse frequency Ω_r/ω	0.123
Reduced longitudinal frequency Ω_l/ω	0.04
Normalized transverse acceptance	1.8 π mm mrad
Ω_l/Ω_r	0.326
Vane length	392 cm

Beam dynamics simulations

The multi-particle code DYNAMION [6] was used for simulating beam dynamics in the RFQ. The electric field acting on each particle is calculated using coefficients of the series (1). The initial particle distribution shown in Fig. 2 was obtained from three-dimensional beam dynamics simulations in the section of LEBT containing the multi-harmonic buncher. Figure 6 shows trajectories of some particles with different initial phases plotted in the same coordinate system as in Fig. 3. Figure 6 presents particle trajectories for stable (solid curves) and unstable (dotted curves) motion. One can see that some particles are captured for the acceleration with amplitudes of longitudinal oscillations which can be even larger than the separatrix size corresponding to a particle moving on the RFQ axis. The fact that trajectories are concentric confirms that the longitudinal motion is adiabatic during the acceleration which follows from condition (2).

The longitudinal phase space portrait of the beam exiting the RFQ is shown in Fig. 7. This plot has a dense core containing 85% of the accelerated particles and a halo. The emittance containing

99.9% of particles is larger than rms emittance by the factor of 10. Numerical simulations are consistent with the analytical approximations. It is clear that longitudinal emittance is a function of transverse emittance (see Fig. 8). The RFQ perfectly separates the accelerated and unaccelerated particles by their energies. The unaccelerated particles will be lost in MEBT. Since the beam energy in the MEBT is low, the heat load due to the lost particles is negligible.

The effective longitudinal emittance containing two charge states, U^{+28} and U^{+29}, is bigger than the emittance for individual charge states due to the slightly different synchronous phases of each charge state. Despite of essential halo formation, the total longitudinal emittance of two-charge state beam is much lower than the acceptance of the following superconducting linac [7]. Moreover, we have found that only the external multi-harmonic bunching and the design discussed above provide this lowest possible longitudinal emittance. The total effective emittance of two-charge state beam does not exceed 2.0 π·keV/u·nsec. The beam dynamics studies in the following superconducting linac show excellent beam properties for a multiple charge state uranium beam [7].

The RFQ is designed for the reference charge-to-mass ratio q/A=28.5/238. The acceleration of charge states 28 or 29 produces a slight mismatched motion in the transverse phase space. Figure 9 shows transverse profiles of the single-charge state $^{238}U^{28+}$ beam along the RFQ and one can observe some modulation of beam envelopes. The envelope $r_{max,28}$ is shown for accelerated particles only. The envelope modulation is determined by the expression

$$\xi = \sqrt{\frac{r^2_{max,28}}{\rho^2_{max,28.5}} \cdot \cdot \frac{1}{\lambda \cdot \varepsilon_n}}$$

and does not exceed 5% for each charge state. There is no transverse emittance growth both for single- and two-charge state beams along the RFQ. The transmission of the accelerated particles is a function of the transverse emittance of injected beam as shown in Fig. 10.

The RFQ is followed by the MEBT which must match a two-charge state beam to the following SRF linac. Our studies have shown [4] that SC solenoids are the best option for the MEBT. Beam waists in both transverse planes at the RFQ exit are preferable for matching to the following axial symmetric focusing channel. The last cell of the RFQ is designed in order to produce these desired beam waists.

Both ends of the RFQ structure considered here have a longitudinal voltage about of ~20 kV on the axis as is inherent in split-coaxial structures. Beam dynamics simulations show that this voltage does not affect the beam parameters. At the low energy end the effect is negligible due to the long radial matching section. At the exit of the RFQ this effect is also small due to the relatively high energy of the particles.

RFQ cavity design

A conventional four-vane RFQ cavity with a longitudinal direction of the magnetic flux in the resonator chambers provides high shunt impedance due to the simple shape, and wide and smooth paths for rf currents. Shunt impedances of most operating four-vane RFQs are close to the calculated ones. However, the four-vane structure is not appropriate in low frequency range due to the large transverse dimensions. In addition a special care must be taken in order to properly separate non-operating modes. A cavity operating in a split-coaxial mode has been proposed and built for RFQs in the ~12-25 MHz frequency range. This type of resonant cavity reduces the transverse dimensions of the cavity significantly compared to the four-vane structure. In addition, the split-coaxial mode provides high stability of the accelerating field because the transverse magnetic field encircles all four vanes as in a coaxial waveguide. Operational experience with a prototype 12 MHz RFQ [8]

does not show any multipacting in full power range from zero to the designed value. This feature is very important for the RFQs assigned for acceleration of various ion beam species.

There are some other examples of operating low-frequency RFQs but all of them have essential disadvantages and selection of the proper RFQ cavity operating at 57 MHz in CW regime is still a challenge. On the basis of our previous experience in developing of low-frequency RFQ cavities [9-12] we propose a new type of RFQ structure which combines the advantages of the four-vane and split-coaxial structures. An isometric view of the full-length computer model of the cavity is shown in Fig. 11. It can be considered to be a hybrid of a conventional four-vane structure with coupling "windows" between the chambers and split-coaxial cavities. The specific magnetic field distribution makes it possible to provide a resonant frequency of 57.5 MHz within a 60 cm diameter tank. This structure provides high shunt impedance, relatively simple mechanical design, moderate diameter and large frequency separation of the operating and non-operating modes. There are both longitudinal and transverse components of the magnetic field with respect to the longitudinal axis: some of the magnetic flux is directed around the axis while some magnetic flux surrounds the stems stabilizing the field distribution in the operating mode. The elliptical shape of the windows provides a low density of rf current on the vane surface and improves the longitudinal flatness of the voltage distribution compared to other low-frequency RFQ structures. In addition, this vane shape provides good mechanical stability and the possibility of a modular design of the RFQ cavity.

The final RFQ cavity is *606* mm in diameter and consists of six *652* mm long modules. The exact dimensions of the cavity and vanes are under optimization from the point of view thermal and structural stability. Preliminary dimensions of the vanes are given in Fig. 12.

Electrodynamics simulations of the cavity has been carried out using the CST Micro-Wave Studio (MWS) [13] and OPERA 3D codes. The main results are presented in Table 3. Rf power losses were calculated taking into account realistic distribution of electrical field between the vanes. The focusing gradient simulated by the MWS code is presented in Fig. 13. The losses have been determined for a design gradient value $G_0 = U_0/R_0^2 = 190$ kV/cm^2. The use of vane-to-vane voltage for the calculation of rf power losses can lead to underestimation of these losses.

Table 3. Calculated electrodynamics parameters of the cavity.

Frequency of operating mode	57.5 MHz
Frequency of the nearest mode	68.4 MHz
Frequency of the second nearest mode	93.5 MHz
Q-factor	12000
Total rf power losses	45 kW
Specific rf power losses	11.5 kW/m

The results of the electrodynamics calculations are used for further finite element analysis of the thermal and mechanical properties of the cavity.

RF voltage variation along the vanes is an inevitable property of any longitudinally non-uniform structure. In our case the magnitude of the voltage variation depends mostly on the longitudinal size of the window: the longer the section at the given diameter, the larger the voltage variation. At the same time, the elliptical shape of the window reduces the field variation compared to a rectangular window. One should note that the highest voltage deviation occurs at the ends of the vanes where a additional capacitance between the vanes and the endplate exists. Figure 14 shows a distribution of transverse component of the electric field along the cavity. The spacing between the vane edge and

endplate is 30 mm. The maximum deviation of the field along the cavity is ± 1.3%. The voltage variation within a module is ± 0.23%. The radial matching section of the RFQ can also perturb the voltage flatness. However, a final uniform field distribution along the RFQ may be obtained using standard water-cooled slug tuners.

One of the main parameters of any RFQ cavity is the sensitivity of the rf field distribution to misalignment of the vanes. In order to estimate the influence of the electrode misalignment introduced by an asymmetry in the cavity, simulations with the 3D OPERA code have been carried out. The following relations were found for voltage and frequency deviations as a function of radial displacement of the vane:

$$\frac{\Delta U}{U}[\%] = -6.7\Delta r[\,mm\,] \,, \quad \frac{\Delta f}{f} = 0.009\Delta r[\,mm\,] \,.$$

The voltage and frequency deviations can be controlled by requiring reasonable tolerances of the vane displacement which should be less than ±100 μm.

Conclusion

A 57.5 MHz CW RFQ for the RIA driver has been designed to ensure stable CW operation and formation of high-quality beams containing two charge states. The beam dynamics have been designed to obtain the specified two-charge state beam parameters maintaining relatively low peak electric field on the vane surface (1.25 kilpatrick). The RFQ forms low longitudinal emittance two-charge state beams without any emittance growth in the transverse phase planes.

A new resonant structure has been developed for the RFQ. It combines advantages of the conventional four-vane and split-coaxial structures. Three-dimensional electrodynamics simulations confirmed that this RFQ structure has high shunt impedance and large frequency separation of the modes.

Fabrication of both a low power "cold model" of the complete RFQ and a single segment "engineering model" is planned for the near future.

References

1. K. W. Shepard, et al., SC Driver Linac for a Rare Isotope Facility, in the Proceedings of the 9th International Workshop on RF Superconductivity, Santa Fe, New Mexico, 1999, pp. 345-351.

2. A.A. Kolomiets et al, RFQ Design Code DESRFQ. ITEP Internal report, Moscow, 1998.

3. A.I. Balabin, Numerical calculation of field in RFQ structure, Preprint ITEP – 107, 1981.

4. P.N. Ostroumov et al, Heavy Ion Beam Acceleration of Two Charge States from an ECR Ion Source, in Proceedings of the XX International Linac Conference, Monterey, California, August 21-25. SLAC-R-561, v.1, p. 202.

5. I.M. Kapchinskiy, Theory of Linear Resonant Accelerators, Moscow, Energoizdat.1982 (In Russian).

6. A.A. Kolomiets, et al., DYNAMION – the Code for Beam Dynamics Simulations in High Current Ion Linac, Proc. of the Sixth European PAC, Stockholm, Sweden, June 22-26, 1998.

7. P. N. Ostroumov Heavy-Ion Linac development for the U.S. RIA Project. Proceedings of this conference.

8. K.W. Shepard, et al, Beam Tests of the 12 MHz RFQ RIB Injector for ATLAS. Proceedings of the 1999 IEEE Particle Accelerator Conference, NYC, 1999, p. 955.

9. V.A. Andreev, G. Parisi, 90^0-apart-stem RFQ Structure for Wide Range of Frequencies, Proc. 1993 Particle Acc. Conf., Washington D.C., May 17-20, 1993, pp.3124-3126

10. V.A. Andreev, A. Kolomiets, S. Yaramishev, J. Klabunde, "Low frequency High Duty Cycle Heavy Ion RFQ", Proc. Linac'94, Tsukuba, Japan, August 1994.

11. V.A. Andreev, et al. Development of the ITEP 27 MHz Heavy Ion RFQ, Proc. of the Int. Particle Accelerator Conf. PAC-97, Vancouver, Canada, May 1997, p.1090.

12. D. Kashinsky, at al. Proc. of the Seventh European Particle Accelerator Conf. EPAC-2000. Vienna, p.854.

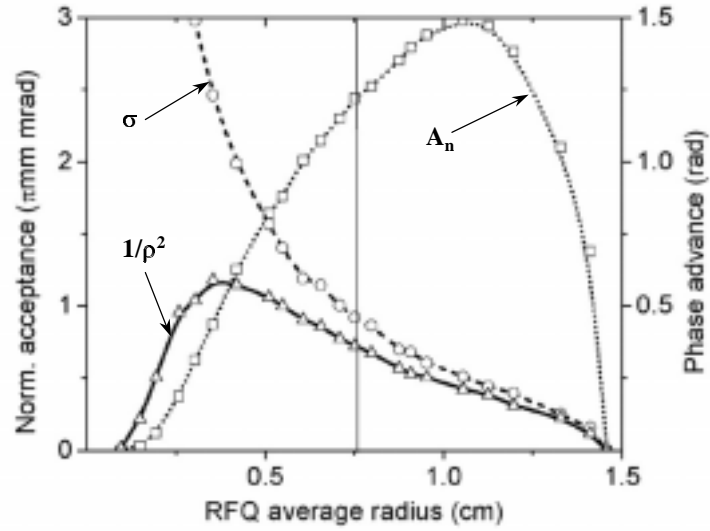13. CST Microwave Studio, User Manual Version 3.0, January 2001, CST GmbH, Darmstadt, Germany. http://www.cst.de/.

Figure 1. Normalized acceptance A_n (dotted line) and transverse phase advance σ (dashed line) calculated for the surface field $E_{max}=140\ kV/cm$. The solid curve represents the parameter $1/\rho_{max}^2$, where ρ_{max} is the maximum value of the modulus of the Floquet function.
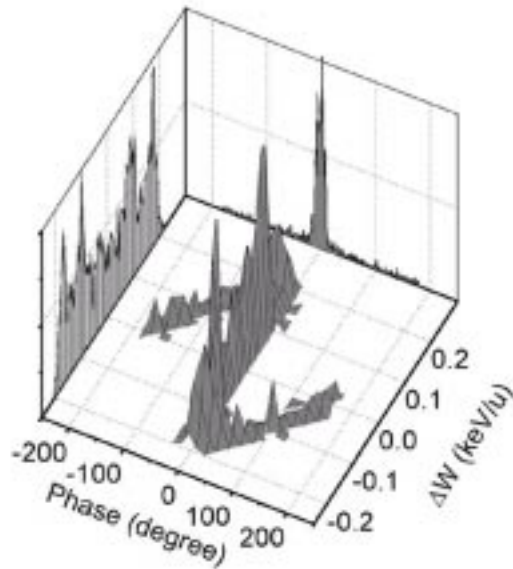
Figure 2. Longitudinal phase portrait of a single charge state beam at the RFQ entrance.
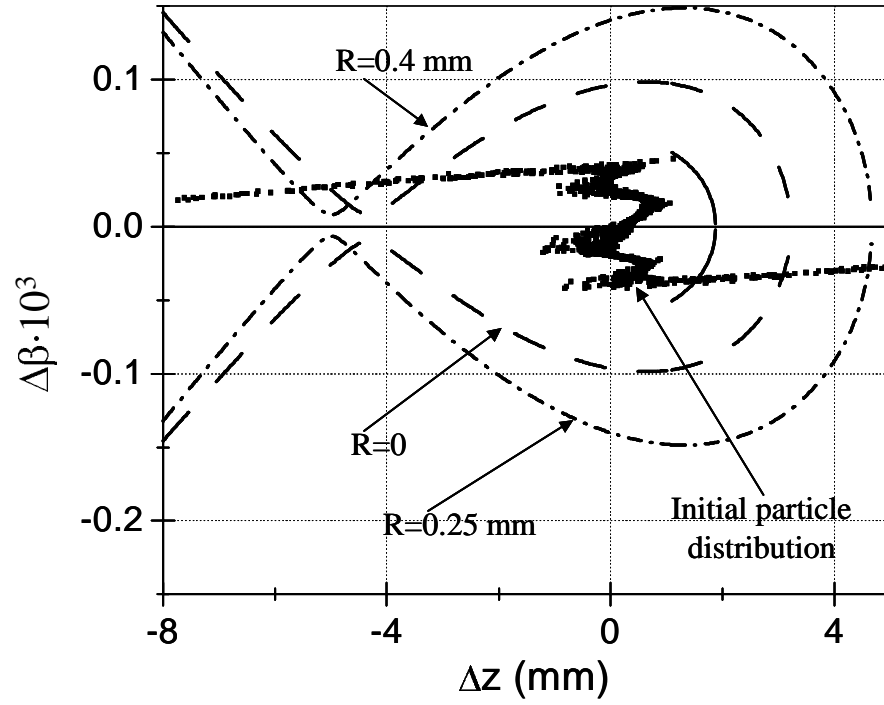
Figure 3. Separatricies of the longitudinal motion at $\beta = 0.00507$ calculated for different amplitudes of transverse oscillations.
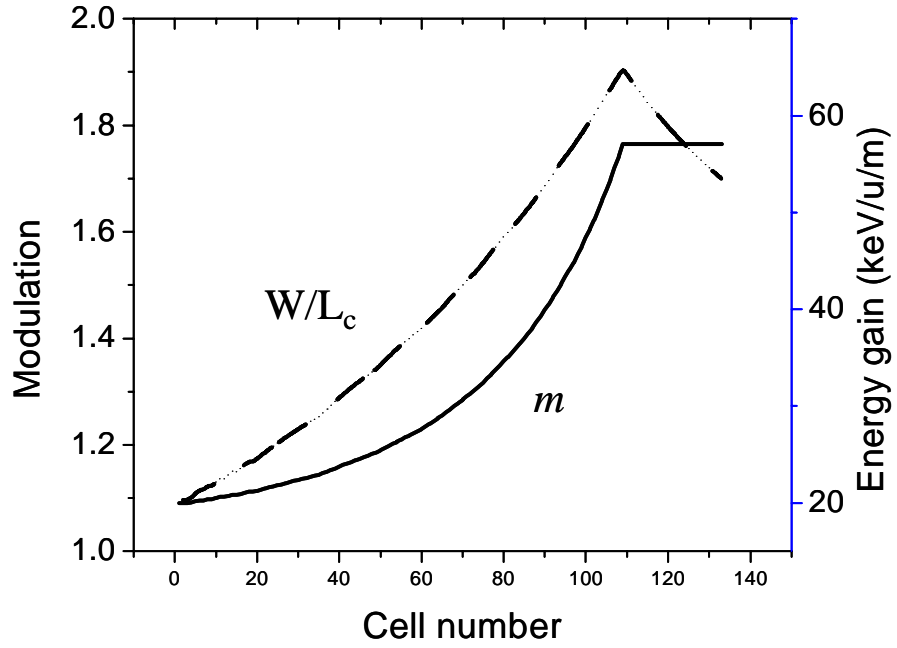
Figure 4. Modulation factor, m, and energy gain, W/L_c, along the RFQ.
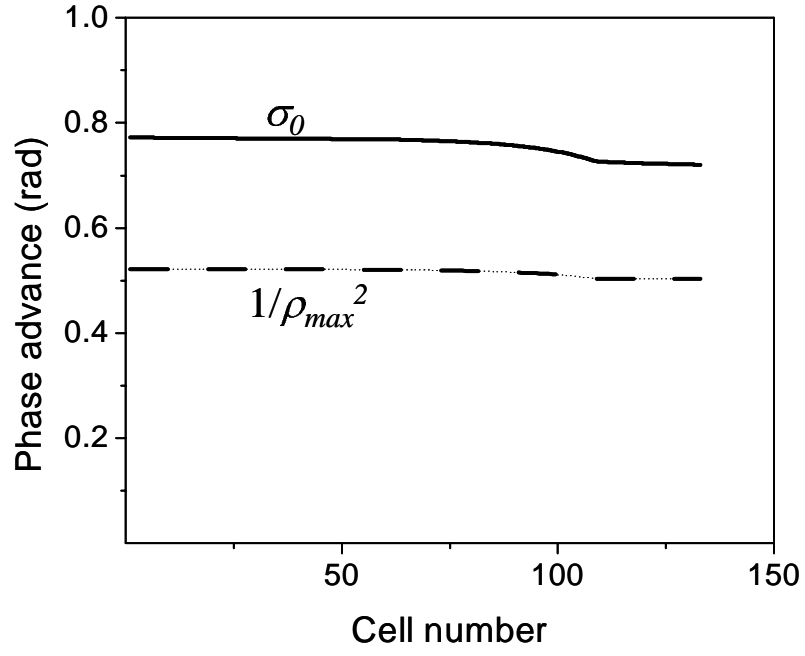
Figure 5. Phase advance, σ_0, and minimum of normalized transverse frequency, $1/\rho_{max}^2$, along the RFQ.
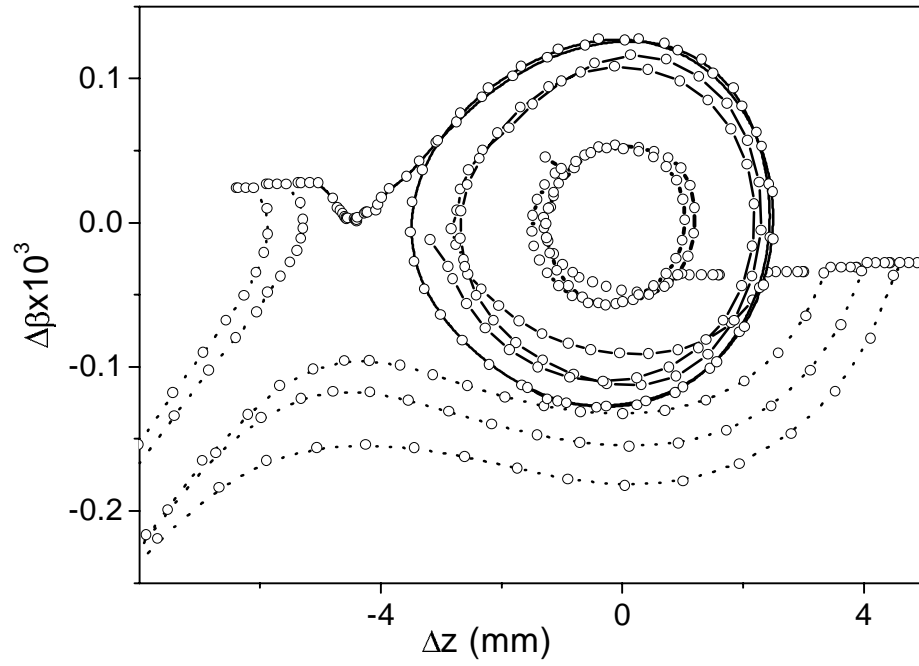
Figure 6. Particle trajectories in the longitudinal phase space. The solid curve represents central trajectories and the dotted curve is for the peripheral particles.
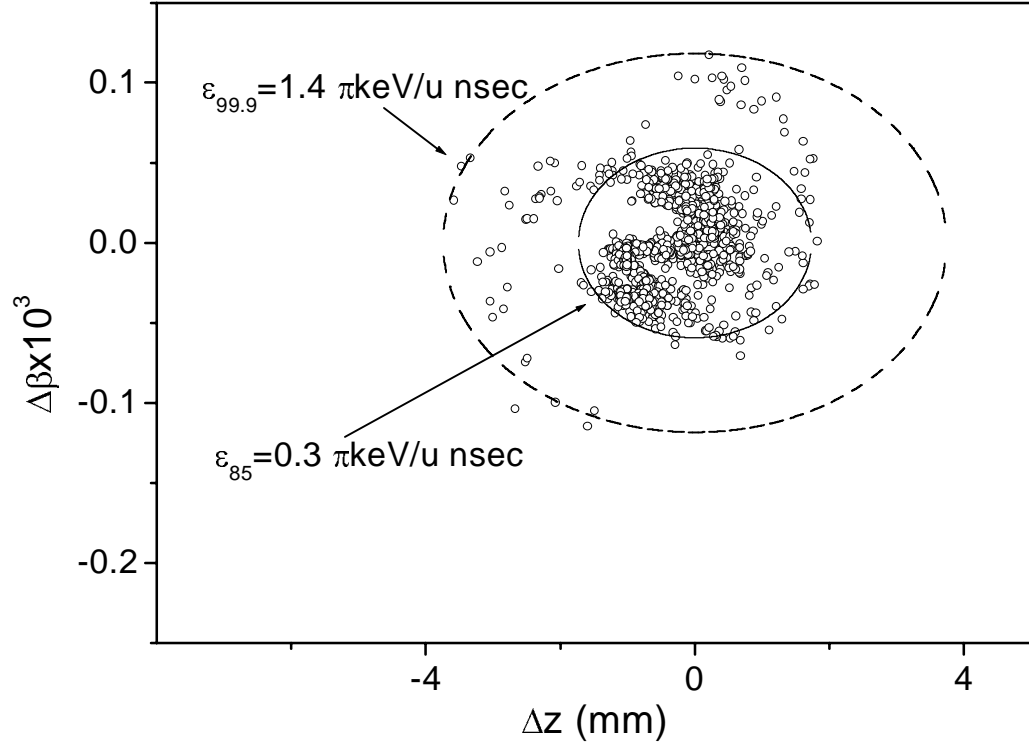
Figure 7. Longitudinal phase space plots of particles exiting the RFQ.
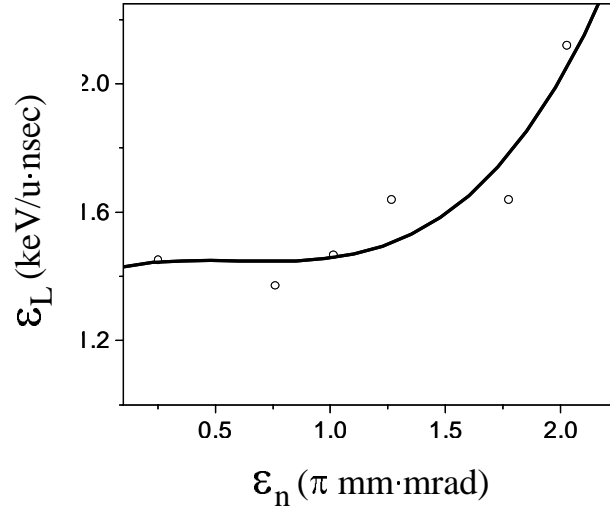
Figure 8. Longitudinal emittance of 99.9% of the accelerated particles, ε_L, in the RFQ as function of input transverse emittance, ε_n.
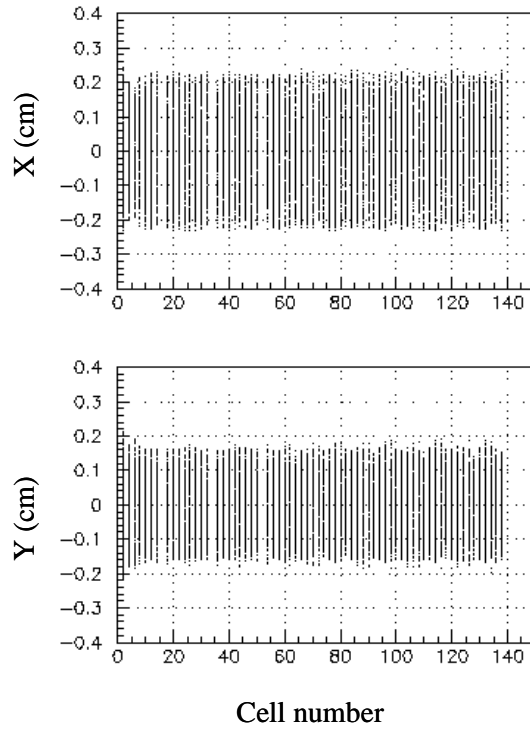
Figure 9. Particle distributions in the transverse planes along the RFQ.
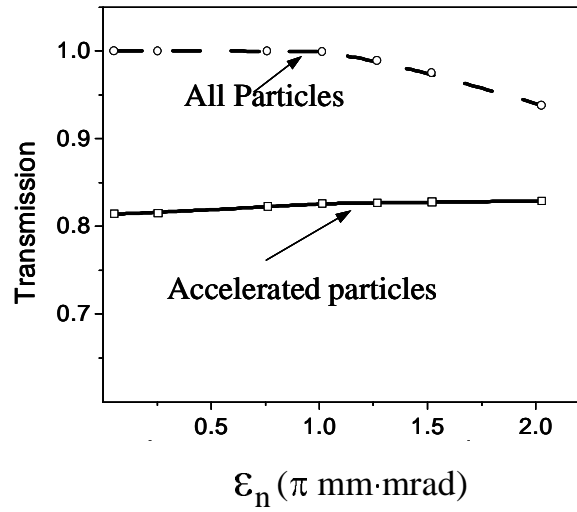
Figure 10. Transmission as function of the input transverse emittance.
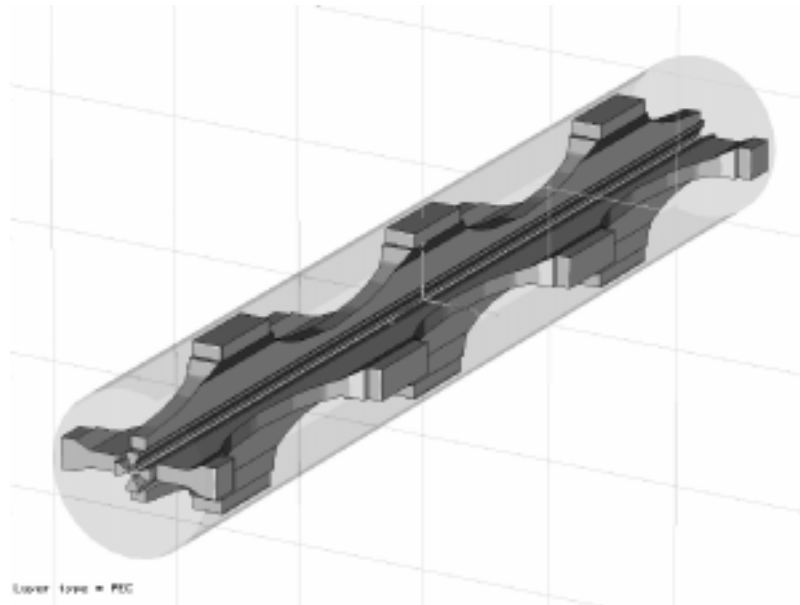
Figure 11. Full length model of the RFQ cavity designed using the MWS code.
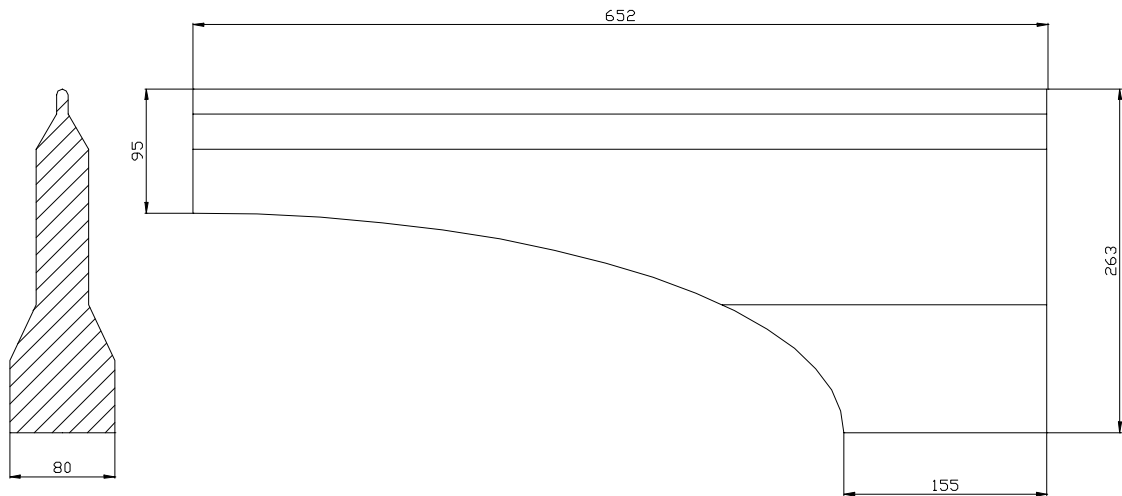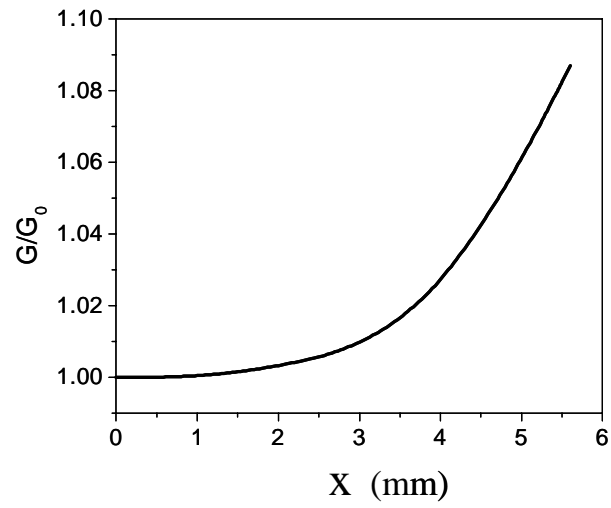

Figure 12. Sketch of the vane.

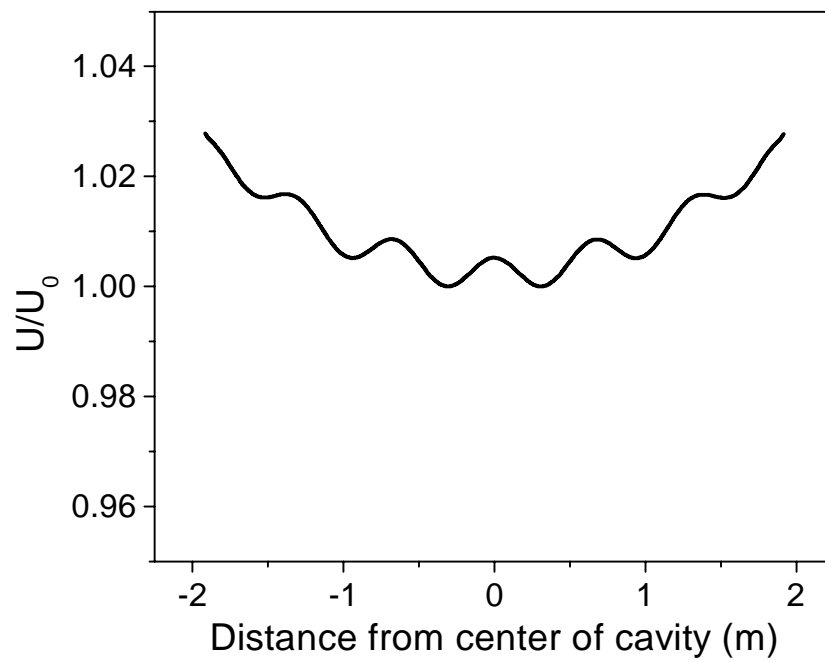Figure 13. Gradient of the electric field as a function of transverse distance.

Figure 14. Transverse electric field along the RFQ with unmodulated vanes.